4th Specialty Conference on Coastal, Estuary and Offshore Engineering
4e Conférence spécialisée sur l'ingénierie côtière et en milieu maritime

Montréal, Québec
May 29 to June 1, 2013 / *29 mai au 1 juin 2013*

WAVE PROPAGATION AND GROWTH IN THE KINGSTON BASIN OF EASTERN LAKE ONTARIO

Matthew P. McCombs[1], Ryan P. Mulligan[1], Leon Boegman[1], and Yerubandi R. Rao[2]
[1]Department of Civil Engineering, Queen`s University, Canada
[2]Environment Canada, Water Sciences & Technology, National Water Research Institute, Canada.

Abstract: The spectral wave model SWAN (Simulating Waves Nearshore) has been used to understand the wave dynamics in the Kingston Basin of Lake Ontario. The model was validated by comparing field observations with numerical simulation results. Two storm events were modelled over the complex bathymetry of the Kingston Basin and wave results were compared to acoustic wave gauges collected over the 2009-2010 and 2011-2012 winter periods. The model was forced with forecast data from the Great Lakes Coastal Forecasting System (GLCFS) and a meteorological station on Simcoe Island. The focus of this study is the validation of the wave simulations and to gain an understanding of the wave field during storm events. SWAN was able to produce a significant wave height root-mean-squared error (RMSE) of 0.26m and a wave period RMSE of 0.93s during a storm event. A validated model resulted in significant wave heights inside the Kingston Basin of up to 3.5m with wave periods of 7s composed of both swell and wind-sea. The swell waves entering the Kingston Basin lose approximately 17% energy density due to the natural barrier on the western rim of the Kingston Basin called Duck-Galloo Ridge. Future work will extend the model to determine the potential environmental impacts of offshore wind farm construction in the region.

1 INTRODUCTION

State-of-the-art wave models solve the spectral action balance equation using source terms such as wind stress, three-wave interactions, four-wave interactions, and dissipation (wave breaking, whitecapping, and bottom friction). The wave model SWAN (Booij et al. 1999) is used in this study to simulate the wave field through the Kingston Basin (the northeastern portion of Lake Ontario and headwaters of the St. Lawrence River). SWAN has been used in other studies to simulate waves over steep and complex bathymetry. As an example, Gorrell et al. (2010) found that SWAN accurately predicted the propagation of observed gravity waves to the shoreline over complicated nearshore bathymetry that included a steep submarine canyon in California. The Kingston Basin (Figure 1) is also composed of complicated topography including many islands and shoals protecting it from large waves in the main basin of the lake (Sly and Prior, 1984). Two deep channels exist around these islands which affect wave propagation. The channel on the east side of Main Duck Island (see Figure 1) is named the Saint Lawrence Channel and on the west is the Simcoe Island Channel. The Saint Lawrence Channel reaches 56.2m in depth and the Simcoe Island Channel reaches 41.2m in depth. The shoals and islands which protect the Kingston Basin form Duck-Galloo Ridge, which averages at a depth of approximately 15m.

Flow distribution and circulation through the Kingston Basin have been described by Tsanis et al. (1990, 1991) and modelled by Paturi et al. (2012). Shore (2009) modeled the flow through Lake Ontario and identified the seasonal flow regimes affecting the Kingston Basin. Bottom sediments in the Kingston Basin

have been studied by Gilbert (1999) who defined three sediment environments and found that the sediment distribution throughout the basin was primarily affected by wave energy. Although seasonal flows have been well documented, the wave field during storm events is not well understood.

The purpose of this paper is to validate the SWAN model and use the predictions to understand the wave field through the Kingston Basin. This will be the first step towards numerically modelling the impact of a proposed offshore wind farm on waves and currents through the Kingston Basin. The wave field is described by comparing water depth and wave energy density from the main basin of Lake Ontario and eastward through the Kingston Basin towards the head of the St. Lawrence River.

2 OBSERVATIONS

The model was forced with wave data from the Great Lakes Coastal Forecasting System (GLCFS; Schwab, 1994) at site D (location of the NDBC Prince Edward Point Buoy) along the southern boundary and compared with field observations within the Kingston Basin and along the Duck-Galloo Ridge (Figure 1). The waves simulated by the GLCFS at site D, the location of the Environment Canada Prince Edward Pt. buoy (not deployed in the winter months), were presumed to be a good representation of wave conditions across the southern boundary. Observational data was collected over two winter periods. The 2009-10 winter observations were made using a Nortek AWAC (acoustic wave and current profiler, Figure 1, site A); data was provided by W.F. Baird & Associates Coastal Engineering Ltd., which captured two storm events (Figure 2, AS1 and AS2). These two events were simulated to ensure accurate representation by the model of the waves at Duck-Galloo Ridge outside the basin. The 2011-12 winter observations were made with an RDI ADCP (acoustic Doppler current profiler) at site B, and RBR TGR and TWR (pressure sensors) deployed by Environment Canada (at sites B and C, respectively). During this period a meteorological station was located at Nine Mile Point on Simcoe Island (site M) and the wind observations were used to force the model for the 2011-12 winter storms (Figure 2, BS1, BS2 and BS3). These events were validated to ensure accurate representation by the model of the waves inside the Kingston Basin (site B).

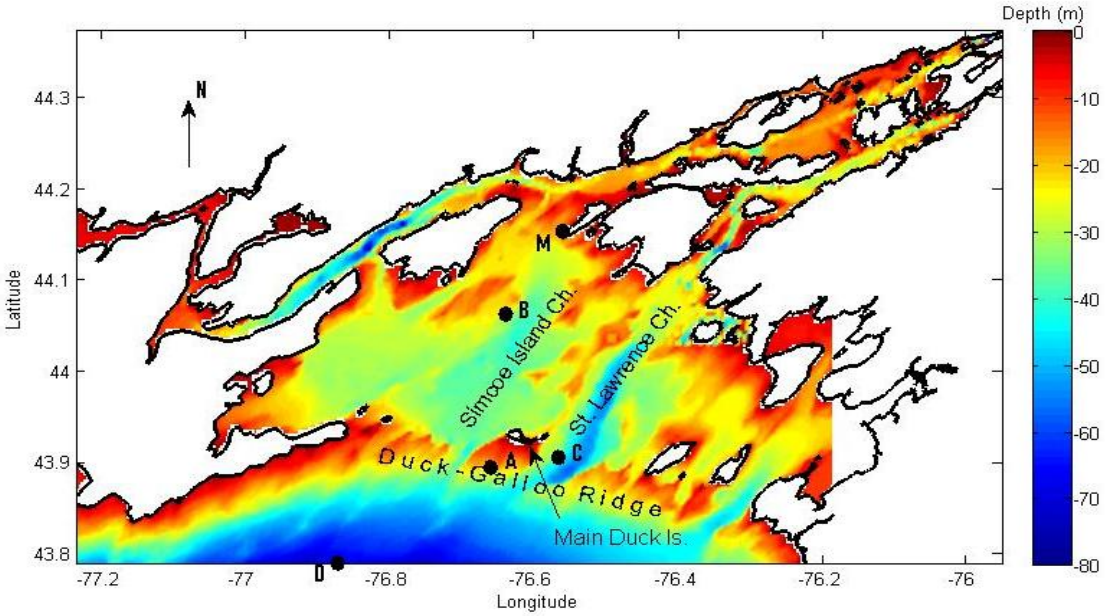

Figure 1: Bathymetry of eastern Lake Ontario (Kingston Basin and St. Lawrence River) based on Lake Ontario Datum (NOAA) and measurement locations: A. AWAC (1.2MHz) for the 2009-10 winter period at a depth of 18m. B. ADCP (600kHz) and TGR for the 2011-12 winter period at 26 m. C. TWR (4Hz) for the 2011-12 winter period at 42m. D. Wave input location from NOAA Great Lakes Coastal Forecasting System at 68m depth. M. Meteorological Station on Simcoe Island.

Wind and wave forcing came from the GLCFS including significant wave heights, H_s, wave period, T_p, and wave direction, θ_p. The GLCFS time series (D) as well as AWAC (A) and ADCP (B) observations of significant wave height for the two winter periods observed are shown in Figure 2. In this study, storms AS2 and BS3 are compared and used to understand the wave conditions inside and outside the Kingston Basin. The wind and wave inputs for the two storms are provided in Figure 3. Strong northwesterly winds of up to 20m/s for storm BS3 produced waves with a significant wave height of up to 4m at the boundary (input from GLCFS at site D) of the model domain. The evolution of peak storm waves through the Duck-Galloo Ridge and into the Kingston Basin is shown and defined in section 4.

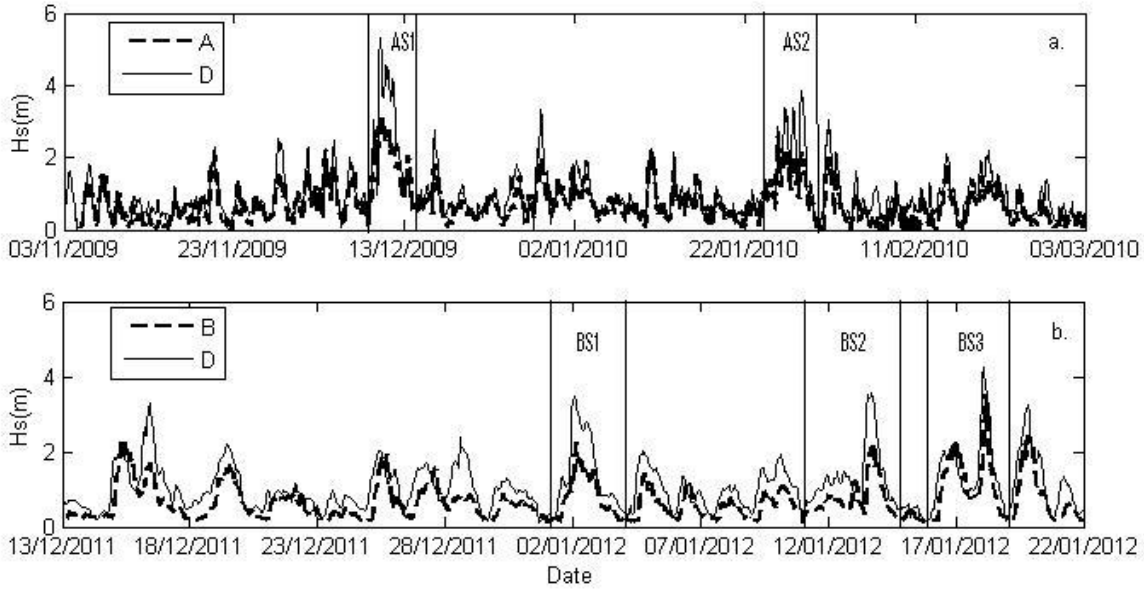

Figure 2: Time series of significant wave height (H_s) for each winter period (a. 2009-10 and b. 2011-12) at various locations (sites A, B, and D). The two storms of interest for this study are AS2 and BS3. Results for the other storms will be presented elsewhere.

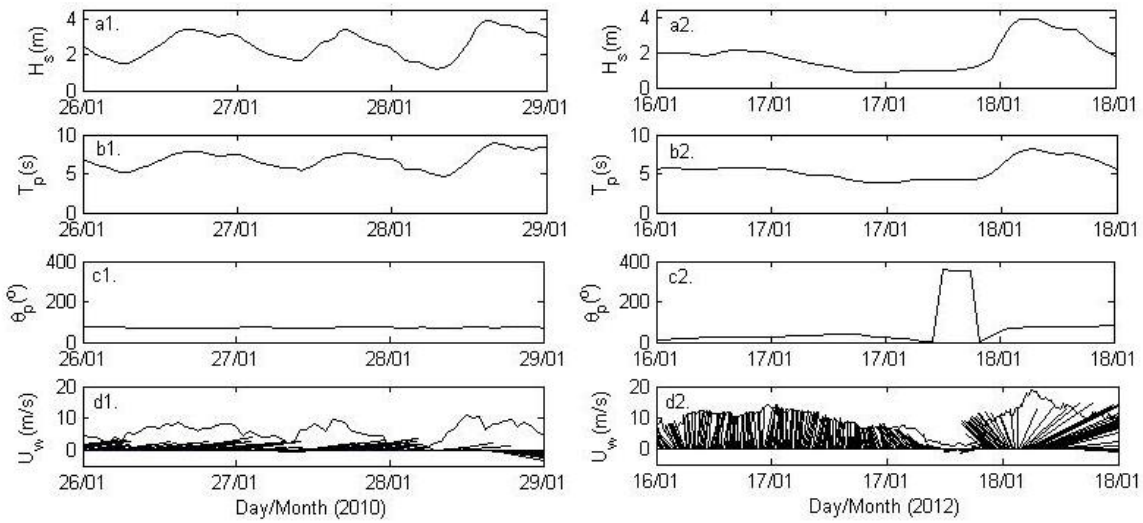

Figure 3: Storm AS2(1) and BS3(2) significant wave height (H_s, a), wave period (T_p, b), wave direction (θ_p, c) and wind speed and wind direction vectors (U_w, d).

3 MODEL SIMULATIONS

The spectral surface wave model SWAN is used to gain an understanding of the surface wave conditions within the Kingston Basin. The SWAN model computes the evolution of random waves and accounts for refraction, as well as wave generation due to wind, dissipation resulting from whitecapping, bottom friction and depth-induced wave breaking and non-linear wave-wave interactions (Booij et al. 1999). The evolution of the wave field is described by the action balance equation (Equation 1). This computation provides its user with the propagation of wave action density in each dimension on the left-hand side and is balanced by local changes to the wave spectrum on the right-hand side:

$$[1] \qquad \frac{\partial}{\partial t}N+\frac{\partial}{\partial x}c_x N+\frac{\partial}{\partial y}c_y N+\frac{\partial}{\partial \sigma}c_\sigma N+\frac{\partial}{\partial \theta}c_\theta N=\frac{S_{tot}}{\sigma}$$

where t is time, c_x and c_y are spatial velocities in the x and y components, c_g is group velocity (speed at which wave action is transported), c_θ and c_σ are rates of change of c_g which describe the directional (θ) rate of turning and frequency (σ) shifting due to changes in currents and water depth, N is wave action density, and S_{tot} are the energy density source terms which describe local changes to the wave spectrum. The energy density source terms include wind, dissipation (whitecapping, bottom friction and depth-induced breaking) and nonlinear interactions (triads and quadruplets). SWAN was run with wave input along a boundary across the portion of the lake shown in Figure 1 at latitude 43.8°N. Wind from the MET station (Figure 1, site M) was forced uniformly through the spherical grid which contained grid cells with dimensions of 267m (longitude) and 373m (latitude).

The wave model was validated with regression analysis of significant wave height, and wave period as well as wave spectral comparison of measurements and observations. Figure 4 contains simulated results and observational data to provide a comparison of significant wave height, wave period and wave direction. Storm AS2 resulted in a RMSE (root mean squared error) for significant wave height of 0.32m and an R value (correlation coefficient) of 0.80. For wave period, a RMSE of 1.20s and an R value of 0.71 were observed. Storm BS3 resulted in a significant wave height RMSE of 0.26m and R value of 0.95 and a wave period RMSE of 0.93s and R value of 0.59.

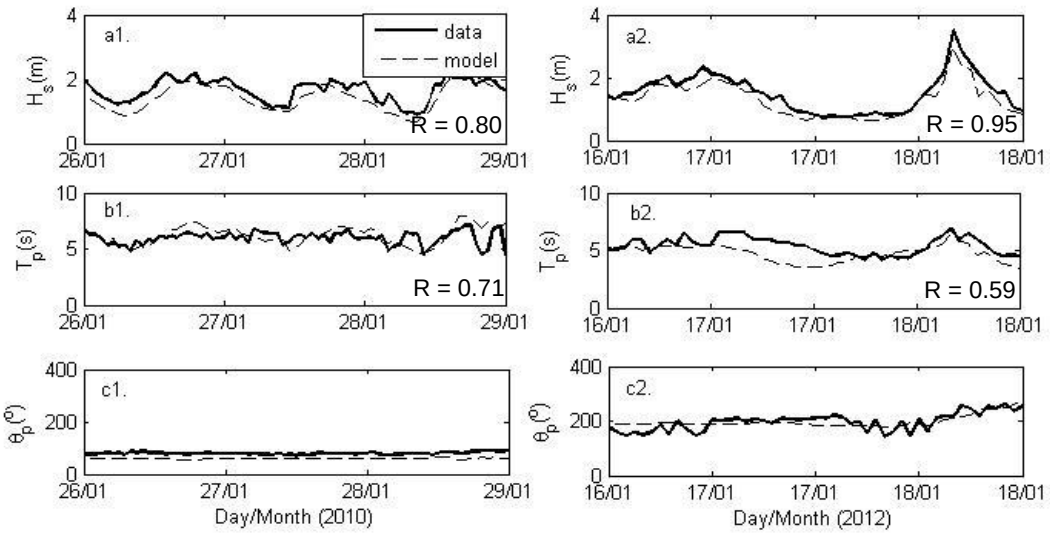

Figure 4: Simulation comparison with observations from the AWAC (site A) for storm AS2 (1) and from ADCP (site B) for storm BS3 (2) of various wave parameters: a. Significant Wave Height (H_s), b. Wave Period (T_p) and c. Wave Direction (θ_p).

The spectral wave comparison of observed waves (Obs) and simulated waves (Mod) is presented for different times at site A (outside the basin) and site B (inside the basin), in Figure 5. The wave spectrum is generally well replicated by the model. Storm BS3 provided better results as the wind data collected and forced into the model was more local and reliable (MET station on Simcoe Island). The number of peaks within the wave spectra is accurately represented by the model after comparison with the observations. At the time of maximum Hs for storm BS3 (Figure 5, b2) one spectral peak occurs in both simulations and observation and two peaks are found in all other times shown. The frequencies at which these peaks occur is not as well represented in storm AS1 although this can be associated with discrepancies in estimated wind input (by GLCFS) to the model for the 2009-10 winter period when compared to measurements by the MET station within the Kingston Basin during the 2011-12 winter period, although both are acceptable inputs to the model which resulted in reasonable errors.

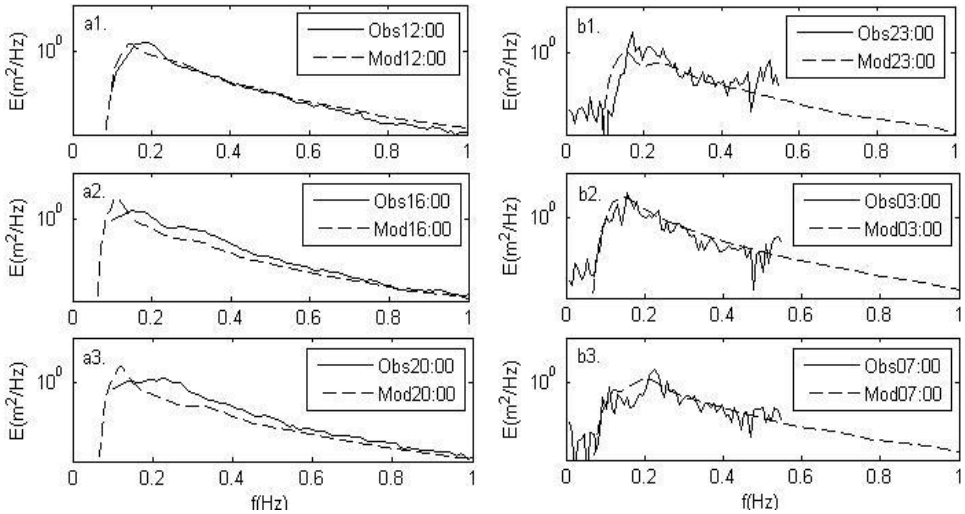

Figure 5: Comparison of surface elevation spectra for observations from the ADCP and AWAC (Obs a and Obs b, respectively) and SWAN (coupled with Delft3D) simulations of storms AS2 (a) and BS3 (b) at storm peaks (2), four hours prior to strom peaks (1) and four hours after storm peaks (3). Peak for AS2 occurs 28/01/2010 and for BS3, 18/01/2012.

4 KINGSTON BASIN WAVE FIELD

The simulated wave field at the peak of storm BS3 is shown in Figure 6. Significant wave height and wave direction vectors throughout the model domain are used to visualize wave progression. In conjunction with Figure 6, to help understand wave progression, is the plot of energy density as waves propagate into the Kingston Basin (Figure 7) and the spectral representations of waves in section 3 (Figure 5).

The spectral representations (Figure 5) suggest that two peaks are generally found in the wave spectrum at sites A and B. The first peak found between 0.1 and 0.2Hz and corresponds to swell waves, implemented at the boundary, moving into and throughout the Kingston Basin from the main basin of the lake. The second peak, between 0.2 and 0.4Hz, represents a transient wind-sea peak from wave growth due to winds over the Kingston Basin. During peak storm conditions (Figure 5, b2), one peak is found within the wave spectrum as winds head in a north-easterly direction perpendicularly to the Duck-Galloo Ridge. The waves at this time are shown in Figure 6 with direction vectors which indicate that the waves at this time travel perpendicularly across the ridge and into the basin resulting in minimal reflection, explaining the single peak in the wave spectra at location B inside the basin in the Simcoe Island Channel. Observations indicate that when winds approach from different directions, waves propagate from the main basin (swell, eg. Figure 5, b2) and new waves are formed within the basin itself (wind-sea, eg. Figure 5, b3). The combination of these two wave types is the cause for the two peaks found in the majority of the spectrum in Figure 5.

The wave field in Figure 6 represents the peak of storm BS3 and indicates the distribution of waves into and throughout the basin. The Duck-Galloo Ridge causes waves to concentrate into the two channels on either side of Main Duck Island. Wave energy is lost crossing the ridge as waves break, shoal, diffract and refract over the islands spanning the ridge. The wave propagation inside the basin is complicated and varies widely throughout. As can be seen in Figure 6, waves rapidly dissipate as they pass over the ridge and refract throughout the model domain particularly in the center of the basin where a windfarm has been proposed.

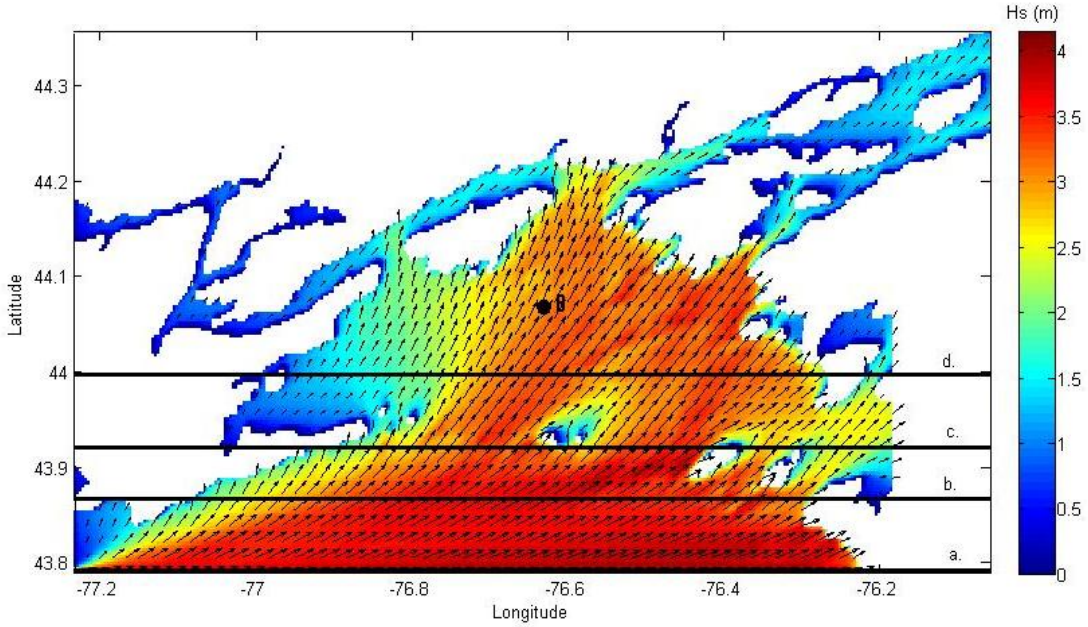

Figure 6: Significant wave height (H_s) and wave direction vectors, whose lengths indicate H_s magnitude, at the peak of storm BS3 (18/01/2012, 03:00). The locations of the four cross-sections referred to in Figure 7 are included (a, b, c and d).

The portion of wave energy (E) which passes over the Duck-Galloo Ridge and into the two channels on each side of Main Duck Island was determined using:

[2] $$E = \frac{1}{8}\rho g H_s^2$$

Where ρ is the density of fresh water, g is acceleration due to gravity and H_s is significant wave height. The energy density at the four cross-sections (Figure 6, a, b, c and d) is provided in Figure 7 with corresponding water depths.

As waves propagate from south to north through the Kingston Basin, a reduction in energy density occurs towards the Duck-Galloo Ridge (Figures 6 and 7, b). Once waves reach the ridge, the energy density is reduced even further as energy is lost in the form of shoaling, breaking, and refracting (Figures 6 and 7, c). In this plot, two of the islands (Main Duck Island and Galloo Island) can be identified where the energy density reduces to zero. The influence of the two islands on the energy density of waves within the basin is less apparent as waves propagate into the Kingston Basin (Figures 6 and 7, d) and shorter period waves are generated by local wind. The largest waves entering the basin lose approximately 17% of their original wave energy density at the boundary due to the influence of the Duck-Galloo Ridge. Energy density continues to diminish as wave energy is lost with the progression of waves through the model domain toward the head of the St. Lawrence River.

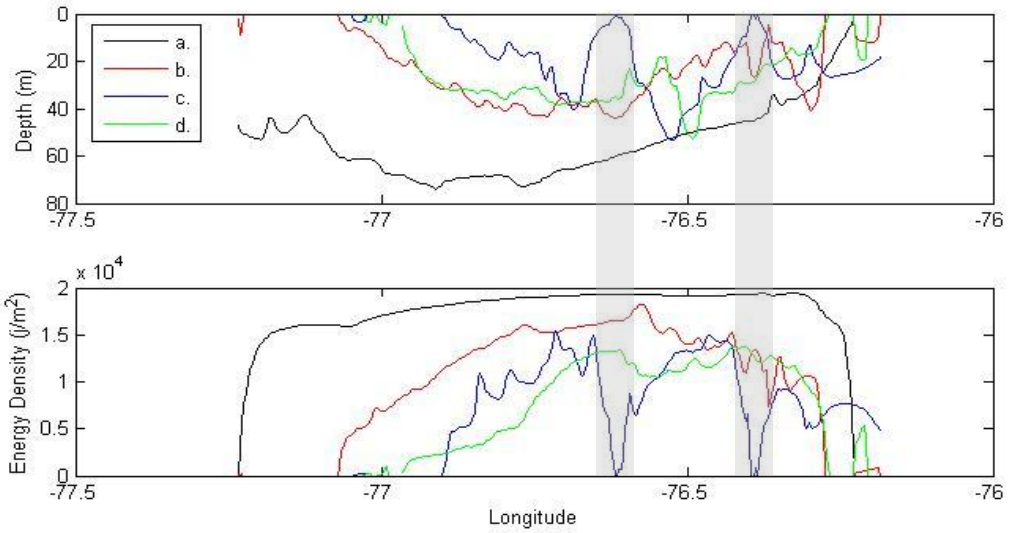

Figure 7: Water depth and wave energy density through cross-sections of the Kingston Basin. The locations of these are shown in Figure 6: a. southern boundary of model domain b. Just outside of Duck-Galloo Ridge in the main basin of Lake Ontario c. Through Duck-Galloo Ridge where the shaded areas represent the locations, along the longitudinal axis, of Main Duck Is. and Galloo Is. d. Inside the Kingston Basin at the peak of storm BS3 (18/01/2012, 03:00).

5 SUMMARY AND CONCLUSION

A spectral wave model was used to simulate two storm wave events through the Kingston Basin in Eastern Lake Ontario, using wave input from greater Lake Ontario on the model boundary and wind-generation of waves over the model grid. This model was validated with observations at two locations collected over two winter periods.

At the peaks of the two storms, we determined that wave propagation from the main basin loses approximately 17% of their energy density due to breaking and refraction over Duck-Galloo Ridge. Within the basin, waves are composed of both swell and wind-sea waves resulting in significant wave heights up to approximately 3.5m and peak wave periods up to 7s. During the largest storms identified, waves are driven by winds perpendicular to the Ridge, causing large waves composed predominantly of swell that enters the basin through Simcoe Island and St. Lawrence channels on both sides of Main Duck Island.

Understanding the wave field in the Kingston Basin will help to determine if the changes in waves due to offshore wind farm construction within the Kingston Basin impact the surrounding area, and may be applicable to future offshore wind farm consideration within the Great Lakes. The flow field, sediment transport and coupling between surface dynamics and temperature stratification will be investigated in future studies.

Acknowledgments

The authors thank Baird and Associates Ltd. for the AWAC observations especially to Andrew McGillis for his helpful suggestions and encouragement. We would also like to thank the crew at Environment Canada for the deployment and retrieval of several instruments used for this study. The main author would also like to thank his supervisors for their continual support and for the sharing of their expansive knowledge and experience. This research was funded by the Ontario Ministry of Research and Innovation Early Researcher Award program.

References

Booij, N., Ris, R.C., Holthuijsen, L.H. (1999). A Third-Generation Wave Model for Coastal Regions 1.Model Description and Validation. *Journal of Geophysical Research*, Vol. 104,pp. 7649-7666: Delft, Netherlands.

Delft-3D User Manual.(2011). *Delft3D-FLOW Simulation of multi-dimensional hydrodynamic flows and transport phenomena, including sediments, User Manual.Deltares*: The Netherlands.

Elias, E.P.L., Walstra, D.J.R., Roelvink, J.A., Stive, M.J.F., Klein, M.D. (2000). Hydrodynamic validation of Delft3D with field measurements at Egmond.Coastal Engineering.

Gorrell, L., Raubenheimer, B., Elgar, S., Guza, R.T. (2010).SWAN Predictions of Waves Observed in Shallow Water Onshore of Complex Bathymetry.Elsevier B.V.: USA

Gilbert, R., Hartling, J.W. (1999). Spacial Distribution of Surficial Sediments in Part of the Kingston Basin of Northeastern Lake Ontario, Canada.NRC: Canada.

Lesser, G.R., Roelvink, J.A., van Kester, J.A.T.M., Stelling, G.S. (2004). Development and validation of a three-dimensional morphological model. *Elsevier B.V*: The Netherlands.

Mulligan, R.P., Hay, A.E., Bowen, A.J. (2010).A wave-driven jet over a rocky shoal. *Journal of Geophysical Research*, VOL. 115, C10038.

Paturi, S., Boegman, L., Yarubandi R. Rao. (2012). Hydrodynamics of Eastern Lake Ontario and upper St. Lawrence River. *J. Great Lakes Res.* VOL. 38, pp. 194-204.

Shore, J.A. (2009).Modelling the Circulation and Exchange of Kingston Basin and Lake Ontario with FVCOM. *Elsevier*: Canada.

Sly, P.G., Prior, J.W. (1984). Late glacial and postglacial geology in the Lake Ontario basin. *Can. J. Earth Sci.* 21. 802-821 (1984).

Schwab, D.J., Bedford K.Q. (1994). Initial implementation of the great lakes forecasting system: A real-time system for predicting lake circulation and thermal structure. *Pollut. Res. J. Can*. 29:2-62-3.

Tsanis, I.K., Masse, A., Murthy, C.R., Miners K. (1991). Summer Circulation in the Kingston Basin, Lake Ontario. *Journal of Great Lakes Research*, Vol. 17, Issue 1, pp.57-73. Elsevier: Canada.

Tsanis, I.K., Murthy, C.R. (1990). Flow Distribution in the St. Lawrence River System at Wolfe Island, Kingston Basin, Lake Ontario. *Journal of Great Lakes Research*, Vol. 16, Issue 3, pp. 352-365. Elsevier: Canada.